Toxicology and Applied Pharmacology 244 (2010) 280–290

Contents lists available at ScienceDirect

Toxicology and Applied Pharmacology

journal homepage: www.elsevier.com/locate/ytaap

Evaluation of two different metabolic hypotheses for dichloromethane toxicity using physiologically based pharmacokinetic modeling for *in vivo* inhalation gas uptake data exposure in female B6C3F1 mice

M.V. Evans [a,*], J.C. Caldwell [b]

[a] National Health and Environmental Effects Research Laboratory, Office of Research and Development, U.S. Environmental Protection Agency, Research Triangle Park, NC 27711, USA
[b] National Center for Environmental Assessment –Washington Division, Office of Research and Development, U.S. Environmental Protection Agency, Research Triangle Park, NC 27711, USA

ARTICLE INFO

Article history:
Received 23 November 2009
Revised 25 January 2010
Accepted 30 January 2010
Available online 10 February 2010

Keywords:
Physiologically based pharmacokinetic (PBPK) model
DCM
Dichloromethane
Methylene chloride
Metabolism
Atypical CYP kinetics

ABSTRACT

Dichloromethane (DCM, methylene chloride) is a lipophilic volatile compound readily absorbed and then metabolized to several metabolites that may lead to chronic toxicity in different target organs. Physiologically based pharmacokinetic (PBPK) models are useful tools for calculation of internal and target organ doses of parent compound and metabolites. PBPK models, coupled with *in vivo* inhalation gas-uptake data, can be useful to estimate total metabolism. Previously, such an approach was used to make predictions regarding the metabolism and to make subsequent inferences of DCM's mode of action for toxicity. However, current evidence warrants re-examination of this approach. The goal of this work was to examine two different hypotheses for DCM metabolism in mice. One hypothesis describes two metabolic pathways: one involving cytochrome P450 2E1 (CYP2E1) and a second glutathione (GSH). The second metabolic hypothesis describes only one pathway mediated by CYP2E1 that includes multiple binding sites. The results of our analysis show that the *in vivo* gas-uptake data fit both hypotheses well and the traditional analysis of the chamber concentration data is not sufficient to distinguish between them. Gas-uptake data were re-analyzed by construction of a velocity plot as a function of increasing DCM initial concentration. The velocity (slope) analysis revealed that there are two substantially different phases in velocity, one rate for lower exposures and a different rate for higher exposures. The concept of a "metabolic switch," namely that due to conformational changes in the enzyme after one site is occupied – a different metabolic rate is seen – is also consistent with the experimental data. Our analyses raise questions concerning the importance of GSH metabolism for DCM. Recent research results also question the importance of this pathway in the toxicity of DCM. GSH-related DNA adducts were not formed after *in vivo* DCM exposure in mice and DCM-induced DNA damage has been detected in human lung cultures without GSH metabolism. In summary, a revised/updated metabolic hypothesis for DCM has been examined using *in vivo* inhalation data in mice combined with PBPK modeling that is consistent with up-to-date models of the active site for CYP2E1 and suggests that this pathway is the major metabolizing pathway for DCM metabolism.

Published by Elsevier Inc.

Introduction

Dichloromethane (DCM, methylene chloride) is a volatile compound used as an extraction solvent in different processes such as the textile and pharmaceutical industries. Prior to the mid-1980s, the main health effects of concern were acute, mainly formation of carboxyhemoglobin and carbon monoxide poisoning. However, concerns about long-term effects have been raised after rodent bioassays indicated inhalation of DCM caused liver and lung cancer in mice (NTP, 1986). IARC (1999) determined the animal data to present sufficient evidence of carcinogenicity in experimental animals based on lung and liver tumors in mice exposed by inhalation and mammary tumors in rats (both sexes) exposed by inhalation. In addition to these tumor sites, there is evidence of relatively rare astrocytoma or glioma tumors at relatively low exposure concentrations in rats. Therefore, DCM has been reported to induce tumors at multiple sites across multiple species and gender (Serota et al., 1986a,b; Hazelton Laboratories, 1983; Maltoni et al., 1988; Mennear et al., 1988; NTP, 1986; Nitschke et al. 1988).

PBPK models in combination with gas-uptake data have been developed to quantify metabolism for volatile compounds (Gargas et al., 1986; Andersen et al., 1994; Evans et al., 2009). One of the major advantages of gas-uptake inhalation data is that they provide time-series data non-invasively. An initial bolus injection of the compound is given at time zero in a closed system. The decline in chamber atmosphere can be directly correlated to total metabolism after accounting for all other variables. PBPK models are useful tools especially for extrapolations across different species or routes of

* Corresponding author. US EPA, MD B143-01, Research Triangle Park, NC 27711, USA. Fax: +1 919 541 4284.
E-mail address: evans.marina@epa.gov (M.V. Evans).

0041-008X/$ – see front matter. Published by Elsevier Inc.
doi:10.1016/j.taap.2010.01.018

exposure. PBPK modeling results of DCM gas-uptake data have led to the hypothesis that there are two metabolic pathways involved in DCM metabolism: one major pathway mediated by P450s, mainly CYP2E1, and another pathway mediated by glutathione (GSH), mainly glutathione S-transferases (GSTs) (Guengerich et al., 2003).

The GSH/GST pathway was then suggested to be that most relevant to the cancers observed in mice and to a much lesser extent in other rodents, as first suggested from PBPK consideration (Gargas et al., 1986) and later suggested by direct mutagenic systems in bacterial assays. Carcinogenic effects of DCM have been believed to be mediated by metabolism in liver and lung (Anders, 2008). The GSH/GST pathway has been hypothesized to contribute to DCM's carcinogenic effects in the liver, as P450 enzymes become saturated with increasing exposure concentrations and metabolism would depend more on the glutathione–transferase pathway. DCM metabolism was suggested to then continue to increase linearly with increasing exposure (Slikker et al., 2004). This metabolic change has been presumed to be an important component of the mode of action (MOA) of this chemical for liver toxicity and assigned to GSH/GST metabolism. The proposed MOA was dependent on the two-pathway metabolism predicted by PBPK modeling.

The proposed two-pathway metabolic scheme for DCM is presented in Fig. 1. As stated above, there is one P450-dependent pathway in which formyl chloride and CO are formed followed by GSH conjugation of formyl chloride. There is an additional and separate pathway for GSH/GST conjugation of DCM directly that does not involve P450 metabolism but primarily metabolism through GST-theta. The P450 pathway and the direct GSH conjugation pathway both form CO and CO_2. Watanabe and Guengerich (2006) studied the oxidation of DCM to formyl chloride in rat and human microsomes, with the addition of GSH after oxidation. In their discussion, these authors state that attributing 30% (Gargas et al., 1986) of formyl chloride clearance to result from GSH conjugation is not tenable and that the reactivity of GSH with formyl chloride is very limited. Therefore all GSH involvement with DCM metabolism is through the other pathway and does not occur after oxidation. In addition, Watanabe and Guengerich (2006) also argued against support for GSH involvement as a rate-limiting step in CO formation, an assertion based on PBPK modeling of deuterated DCM gas-uptake data in mice (Andersen et al., 1994). The possibility that GSH/GST conjugation and DNA adduct formation can still take place through the non-oxidative pathway warranted further investigation. Watanabe et al. (2007) presented a set of experiments directly addressing the formation of DNA adducts of GSH reactive metabolites after *in vivo* exposure of DCM to both rats and mice. Using low detection limits, these authors were unable to detect DCM-related DNA-GSH adducts *in vivo* for mice from any pathway. Given, that many of the assumptions regarding the dependence of the non-oxidative pathway for a potential mode of action were not supported by these recent studies, the question of whether the gas uptake data could support metabolism that does not involve GSH/GST arose. Finally, recent structural information obtained for human CYP2E1 warrants an update for the metabolic scheme of DCM.

Previous PBPK modeling predictions were based on the assumption that all P450s follow typical Michaelis–Menten behavior. This assumption includes CYP2E1, the main isoenzyme that metabolizes DCM. This assumption is based on the belief that the active site for CYP2E1 is very small. Increasingly, several P450s have been shown to deviate from rigorous Michaelis–Menten behavior. Recent studies have shown atypical kinetics for CYP2A6, and CYP2E1 in human Supersomes™ (Harrelson et al., 2007). Harrelson et al. (2007) review the importance of deuterated studies used to reveal structural and mechanistic details for CYPs. Specifically, these authors stated that "CYP2E1 and CYP2A6 are good candidates for comparative studies that focus on the relationship between substrate dynamics and enzyme structure." They note that, in addition to belonging to the same CYP2 family, these P450s share a rather broad overlap in substrate selectivity (e.g., dimethylnitrosamine, diethynitrosamine, *p*-nitrophenol, halothane, acetaminophen, and butadiene) and both are widely assumed to have relatively small active sites because of their preference for low molecular weight substrates. The belief that the active site for CYP2E1 is relatively small and, without multiple binding sites, is relatively widespread. However, data for human Supersome CYP2E1™ have shown atypical kinetics for m-xylene and 7-ethoxycoumarin metabolism (Harrelson et al., 2008). One possible explanation for a metabolic change observed in P450 atypical kinetics is due to two binding sites being simultaneously available at the active site due to a structural change produced by the first substrate (Tracy, 2006). The structural change can be a rotation that can facilitate access of the active site to a second substrate. The metabolic rate equations needed to describe two multiple sites have been reported (Korzekwa et al., 1998) and can be applied to DCM metabolism via gas-uptake data. The major advantage of the two-site model seems to be its ability to explain the metabolic change in rate displayed by DCM at higher concentrations, without the need to change to a different enzyme.

The first PBPK model that included a two-pathway model for DCM metabolism was for rats using gas-uptake data in addition to CO blood level data (Gargas et al., 1986), followed by models for in mice and humans (Andersen et al., 1987). The original DCM PBPK model for rats (and then mice and humans) used estimates of total metabolism

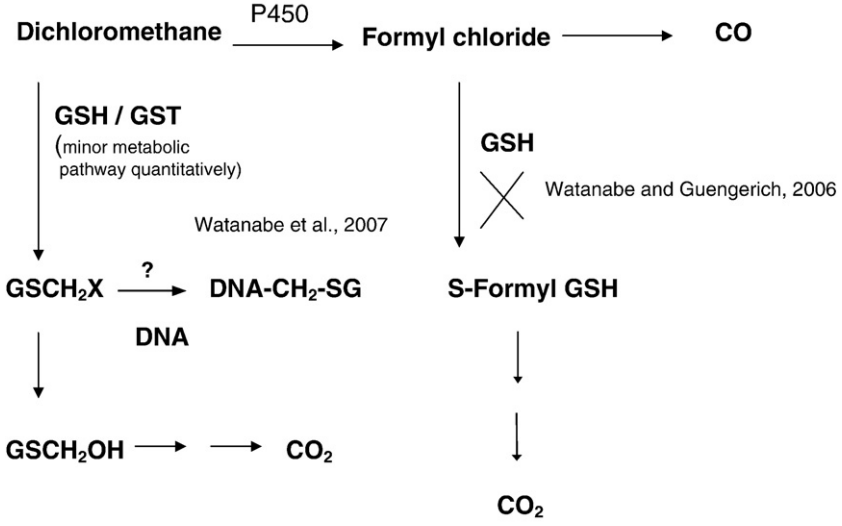

Fig. 1. Updated metabolic scheme for DCM.

assumed to occur in only the liver. More recent DCM PBPK models have also added metabolism in the lung (Sweeney et al., 2004). As stated above, an update of the metabolic scheme may be necessary. In order to be able to compare our results with the original analyses, we decided to assume that total metabolism occurs in the liver. This assumption will enable the direct comparison of the two proposed metabolic hypotheses. The major goals of this paper were (1) to determine if the *in vivo* gas-uptake data in female mice support this alternate metabolic hypothesis for atypical kinetics, specifically due to multiple binding sites for CYP2E1, (2) to re-examine the deuterated *in vivo* gas-uptake data in female mice and its role in supporting a metabolic switching to GSH conjugation after P450 oxidation, and (3) to re-examine the role of PBPK modeling for determination of metabolic pathways assumed to be responsible for DCM effects *in vivo* for mice.

Methods

Gas-uptake data. Inhalation gas-uptake data from available datasets were used to characterize the total rate metabolized by mice exposed to varying initial concentrations of DCM. This type of experiment requires a tight, sealed, or air-closed system where all chamber variables, except for metabolism, are controlled to known set points or monitored. A bolus injection of volatile parent chemical is introduced into the chamber at time zero. The chemical inside the chamber decreases with time as it is absorbed and metabolized by the rodent inside. Chamber concentration measurements are sampled serially for up to 6 h after the bolus injection. Because all other known processes contributing to the decline are quantified, the metabolic parameters for the sum of total metabolism can be determined using regression techniques for the concentration decline. Potentially different metabolic hypotheses can be investigated using a PBPK model that uses gas-uptake-derived metabolic parameters and provides predictions for metabolism that can be tested against *in vivo* data.

There are three major datasets available from the literature and analyzed in this paper: (1) DCM gas-uptake exposures in female B6C3F1 mice (Clewell et al., 1993; Marino et al., 2006), (2) deuterated DCM gas-uptake exposures in female B6C3F1 mice (Andersen et al., 1994; Clewell et al., 1993), and (3) pretreated trans-dichloroethylene (CYP2E1 inhibitor) data in female B6C3F1 mice exposed to an initial concentration of 100 ppm, 1.5 h before start of DCM exposure (Clewell et al., 1993; Marino et al., 2006). Chamber concentration data were the averaged measurement for five mice. All data were digitized using UN-SCAN-IT (Silk Scientific, Orem, Utah, Version 6.0). Graphs of the digitized data were compared visually with the original reported data for QC purposes.

PBPK model structure. The PBPK model for DCM was based on the flow-limited structure described by Ramsey and Andersen (1984) for styrene, as shown in Fig. 2. The organs and compartments included in this version of the model were: lung, liver, fat, and rapidly and slowly perfused compartments. All organs were assumed to be flow-limited. Physiological parameters were obtained from the literature and have been used previously in a PBPK model for gas-uptake of TCE (Brown et al., 1997; Evans et al., 2009), as shown in Table 1. The partition coefficients were chosen specifically for the female B6C3F1 mice as reported previously (Clewell et al., 1993). The differential equations were derived using mass balance principles with the same conditions reported in previous literature (Gargas et al., 1986; El-Masri et al. 2009). The equations were solved numerically using Matlab© (Mathworks, version R2008a), with the ode15s© solver (Mathworks) for integration. This particular PBPK model for DCM predicted total metabolism as measured experimentally from the gas-uptake data in mice. Although previous PBPK models for DCM have predicted total metabolism contributed from both liver and lung (i.e., Sweeney et al., 2004), lung metabolism is typically assumed to be a fraction of that of the liver. However, for the current analysis total metabolism was predicted by the model without distribution between lung and liver.

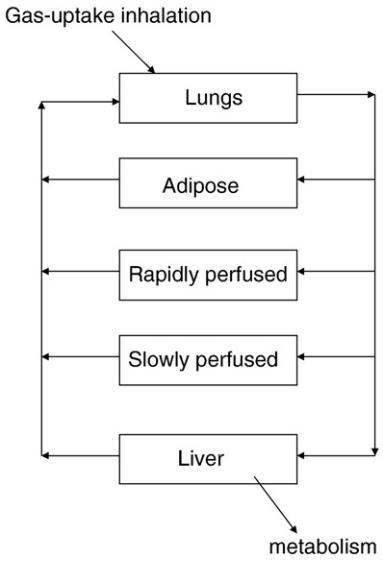

Fig. 2. Schematic representation of PBPK models for DCM. All the organs are the same, with the exception of the liver. Metabolism in the liver is described by either Eq. (1) or Eq. (2) as presented in the text.

Rate of amount metabolized (RAM) modeling. Two different PBPK models were constructed. The models were similar, except for the rate

Table 1
PBPK model parameters.

Abbr.	Parameter description (units)	Baseline value	Source (s)
BW	Body weight (kg)	0.03	(Clewell et al., 1993)
QCC	Normalized cardiac output (l/h/kg)	11.6	(Brown et al., 1997)
VPRC	Ventilation perfusion ratio (unitless)	2.5	(Brown et al., 1997)
QFatC	Scaled fat blood flow (l/h/kg)	0.07	(Brown et al., 1997)
QLivC	Scaled liver blood flow (l/h/kg)	0.161	(Brown et al., 1997)
QSlwC	Scaled slowly perfused blood flow (l/h/kg)	0.217	(Brown et al., 1997)
QRapC	Scaled rapidly perfused blood flow (l/h/kg)	QC − ∑tissue flows	calculated
VFatC	Fat fractional compartment volume	0.07	(Brown et al., 1997)
VLivC	Liver fractional compartment volume	0.055	(Brown et al., 1997)
VRapC	Rapidly perfused fractional compartment volume	0.1	(Brown et al., 1997)
VSlwC	Slowly perfused fractional compartment volume	BW − ∑tissue volumes	calculated
Pbl/air	Blood to air partition coefficient (unitless)	21.8	(Clewell et al., 1993)
Pfat/bl	Fat to blood partition coefficient (unitless)	4.15	(Clewell et al., 1993)
Pliv/bl	Liver to blood partition coefficient (unitless)	1.77	(Clewell et al., 1993)
Prap/bl	Rapidly perfused to blood partition coefficient (unitless)	1.77	Assumed same as liver
PSLw/bl	Slowly perfused to blood partition coefficient (unitless)	0.43	(Clewell et al., 1993)

of amount metabolized equation. The first model used the two-pathway model, whereas the second model used the two-site CYP2E1 model. The two versions of the PBPK model were used to fit the same gas-uptake data. Results for the two metabolic hypotheses were plotted for the regular DCM, deuterated DCM, and trans-DCE pretreatment (i.e., inhibition) gas-uptake experiments.

Two-pathway model. PBPK modeling in combination with gas-uptake data in both rats and mice (Gargas et al., 1986; Clewell et al., 1993) have been used to describe total metabolism by the following two-pathway model:

$$rate = \frac{V_{max}[CV_{Liv}]}{(K_M + [CV_{Liv}])} + k_{gsh} CV_{Liv} V_{Liv} \quad (1)$$

wherein,

V_{max} = maximum velocity of the reaction, mg/h

K_M = affinity constant for the substrate, or concentration at which half maximal velocity is achieved, mg/l

$[CV_{Liv}]$ = venous concentration leaving the liver, mg/l

k_{gsh} = proportionality constant for linear pathway or GSH pathway, /h

V_{Liv} = volume of liver in liters

The use of this particular metabolic hypothesis was based on the assumptions that the major enzyme metabolizing DCM at low concentrations was CYP2E1 (Guengerich et al., 1991), that this enzyme had one single binding site that activates the enzyme, and that the enzyme kinetics are described by typical Michaelis-Menten kinetics. The typical Michaelis-Menten hyperbola shows saturation at higher exposure concentrations and is not sufficient to explain the linear increase in DCM metabolism observed with increasing exposure concentrations. Subsequently, the linear portion of DCM metabolism was assigned to a metabolic switch to GSH metabolism.

One-pathway model via CYP2E1. The linearity of the rate of metabolism at higher exposure concentrations can be described by metabolic switching without the requirement of two different enzymes or metabolic pathways. Metabolic switching can also be described using two separate binding sites within one active site, by using different V_{max}/K_M ratios, as illustrated in Fig. 3. The metabolic rate equations for this type of switch have been developed by Korzekwa et al. (1998) and are in the two-site model that assigns CYP2E1 as the enzyme responsible for DCM metabolism:

$$rate = \frac{V_{max1}[CV_{Liv}] + C_{L2}[CV_{Liv}]^2}{K_{M1} + [CV_{Liv}]} \quad (2)$$

wherein,

V_{max1} = maximum velocity of the reaction for the first binding site, mg/h

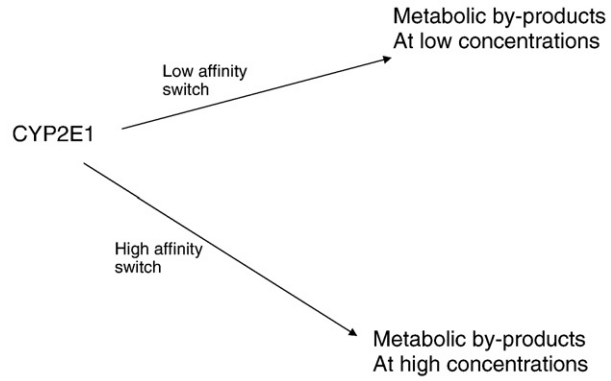

Fig. 3. Two-site metabolic hypothesis for revised model.

K_{M1} = affinity constant for the substrate, for the first binding site, mg/l

$[CV_{Liv}]$ = venous concentration leaving the liver, mg/l

$C_{L2} = V_{max2}/K_{M2}$ ratio for second binding site, l/h, where we assumed $K_{M2} >> K_{M1}$. At low doses, this equation is linear and proportional to V_{max1}/K_{M1}. Similarly, at high doses this equation is also linear, and proportional to $V_{max2}/K_{M2} = C_{L2}$.

Calculation of velocity from gas-uptake data. Gas-uptake experiments are traditionally linked with PBPK models to obtain metabolic estimates using statistical regression techniques. Gas-uptake experiments consist of time-course data collected over the exposure time. This type of time-series data uses the integrated form of the Michaelis–Menten equations to solve for the metabolic parameters. This approach has been adopted from enzyme kinetic work, where the integrated form of the Michaelis–Menten equation has been applied (Atkins and Nimmo, 1973). Another approach that compliments the estimation of metabolic parameters is the direct use of rate equations instead of its integrated time-series form. In this case, the kinetic experiment is performed using increasing substrate doses and always stopped at the same reaction time. The rate or velocity (slope) is then plotted as a function of increasing substrate and is described by a hyperbola for substrates following Michaelis–Menten kinetics. Different regression techniques can then be used to obtain metabolic estimates, such as V_{max} and K_M. Variations on these velocity plots offer different advantages in terms of potential accuracy of the final estimates (Segel, 1993). One of the novel contributions of this paper is to adopt the use of velocity plots in the estimation of metabolic parameters in addition to the traditional time-series approach. Although the same time-course data are used, the results are different. The application of velocity plots is increasingly being used to determine the difference between typical and atypical Michaelis–Menten kinetics (Tracy, 2006).

The slope for the decline in gas-uptake chamber concentration was calculated after the first hour of exposure because distribution and not metabolism is thought to be the predominant effect during this time. All experimental data points between 1 and 2 h were analyzed using Excel's linear regression option (Excel 2003, version 11.8307.8221, Microsoft Office©). The calculated slopes (in ppm/h) were plotted against the initial exposure concentration in ppm. The range of exposures varied between 500 and 5000 ppm. The same analysis was performed for the gas-uptake data using deuterated DCM.

Comparison of two different metabolic models. Several metabolic parameters were optimized for each gas-uptake set using several initial concentrations. The natural log of the gas uptake air concentration was used for all optimizations performed using Matlab's© *fminsearch* tool (Mathworks, version R2008a). For the two-pathway model, three parameters were optimized using the H-DCM and D-DCM datasets: V_{max}, K_M, and k_{gsh}. For the two-site model, there were also three parameters optimized: V_{max1}, K_{M1}, and C_{L2}. After optimization, both models were run with repeated values for initial concentration (C_0) varying between 500 and 5000 ppm at 40 ppm intervals. The simulation results obtained were for the rate of amount metabolized. The rates of metabolism predicted by the two models were plotted against initial chamber concentration.

Results

The modeling results for both metabolic hypotheses are presented in Tables 2 and 3, respectively. Each metabolic model had three parameters that were estimated from fits to the gas-uptake data as presented in Figs. 4–6. Both models provided similar values for the metabolic parameters, except for the rate of amount metabolized as exposure concentration increased. For the two-pathway model, this value is represented by the metabolic rate for GSH, and for the two-

Table 2
Modeling results for both H- and D-DCM.

Modeling variable	Description	Calculated value
Modeling results for the two-pathway model for H-DCM data		
V_{max}	Maximal metabolic velocity, mg/h	1.4
K_M	Affinity constant, mg/l	0.93
k_{gsh}	GSH proportionality constant, /h	0.011
Modeling results for the two-pathway model for D-DCM data		
V_{max}	Maximal metabolic velocity, mg/h	1.65
K_M	Affinity constant, mg/l	10.0
k_{gsh}	GSH proportionality constant, /h	0.1
Modeling results for two-site model with one-pathway for H-DCM data		
V_{max1}	Maximum velocity for first binding site, mg/h	1.3
K_{M1}	Affinity constant for first binding site, mg/l	0.77
C_{L2}	V_{max}/K_M for second binding site, l/h	0.002
Modeling results for two-site model with one-pathway for D-DCM data		
V_{max1}	Maximum velocity for first binding site, mg/h	0.72
K_{M1}	Affinity constant for first binding site, mg/l	2.8
C_{L2}	$V_{max}/K_M$for second binding site, l/h	0.012

site model, the constant reflects clearance by metabolism through the second binding site. Clearance of DCM through the second binding site in the one-pathway model was much lower when compared to that of metabolism through the GSH pathway in the two-pathway model. However, both models resulted in similar fits to the gas-uptake data (Fig. 4). These results indicate that it is not possible to distinguish between the two metabolic models using time-course data from gas uptake.

The modeling results for the deuterated data are also presented in Table 2. In this case, all three parameters change for the two different models. The affinity constant (K_M) for the oxidation component in the two-pathway model is numerically higher than the K_{M1} (first binding site) in the two-site model. The metabolic rate (V_{max}) for the oxidation component in the two-pathway model is higher when compared to the metabolic rate (V_{max1}) for the first binding site in the two-site model. Finally, the constant for the rate metabolized as exposure concentration increase is higher for the two-pathway model (k_{gsh}). The resulting fits for the time-course data using the two metabolic models are very similar to each other (Fig. 5). Exposure to deuterated compounds, including DCM, has been used to argue in favor of both the two-pathway and two-site models. In our experience, this is the first time that deuterated DCM gas-uptake data have been analyzed using both hypotheses. This analysis of time-course data for deuterated exposures was not sufficient to distinguish between the two models. However, more importantly, both metabolic models describe the data well.

The modeling results for the trans-DCE pretreated data are shown in Table 3. When compared to naïve DCM exposure (without pretreatment), the two-pathway model described the inhibition data with a decrease in metabolic rate (V_{max}). For the two-site model, both parameters for the first binding site changed with trans-DCE pretreatment. V_{max1} decreased from 1.3 to 0.15 mg/h and K_{M1} increased from 0.77 to 6.0 mg/l. As for other time course data, the resulting fits are equivalent for both metabolic models (Fig. 6).

Table 3
Modeling results for H-DCM after trans-DCE pretreatment.

Modeling variable	Description	Calculated value
Two-pathway model for trans-DCE pretreated data		
V_{max}	Maximal metabolic velocity, mg/h	0.21
K_M	Affinity constant, mg/l	0.94
k_{gsh}	GSH proportionality constant, /h	0.012
Two-site model, one-pathway for trans-DCE pretreated data		
V_{max1}	Maximum velocity for first binding site, mg/h	0.15
K_{M1}	Affinity constant for first binding site, mg/l	6.0
C_{L2}	V_{max}/K_M for second binding site, l/h	0.0034

Accordingly, a different type of analysis is needed in order to distinguish between the two cases. Based on kinetic analysis performed *in vitro* (such as the calculation of V_{max} and K_M), the analysis was extended to include velocity plots. Using the *in vivo* experimental data, the velocity of the reaction (slope of the gas-uptake data per hour) as a function of initial concentration was biphasic for both H-DCM and D-DCM (Fig. 7). In both cases, there was one metabolic rate for an initial exposure <2000 ppm and a different rate for initial exposures >2000 ppm. The velocity plots obtained showed no evidence of saturation at higher concentrations and therefore supported a metabolic switch.

Velocity plots were generated using the two different PBPK models instead of experimental data. These results are shown in Fig. 8 for H-DCM and Fig. 9 for D-DCM. The simulations for H-DCM show a decrease in slope at higher concentrations for both the two-pathway and two-site models. Modeling predictions for deuterated data indicate a more linear slope for velocity or rate of amount metabolized with increasing dose. The current examples demonstrate that analysis of gas-uptake using several differing approaches and data sets cannot distinguish between the two hypothesized kinetic mechanisms, one involving a single enzyme with two binding sites and the other involving two metabolic pathways.

Discussion

Throughout the application of PBPK modeling, hypothesis generation has been considered one of the most valuable applications of PBPK modeling. Due to the role that PBPK modeling has played for the suggestion of metabolic hypotheses for DCM, it seems appropriate to re-examine the gas-uptake data for other potential metabolic hypotheses. Although gas-uptake data quantifies total metabolism, different metabolic hypotheses can be incorporated in the models and used with gas-uptake data to evaluate its internal consistency with the model. At the time that the initial PBPK models were published (mid to late 1980s), the active site for CYP2E1 was considered to have only one binding site. Any chemical metabolized by CYP2E1 could be then calculated by the Michaelis-Menten equation for rate metabolized. Given this mechanistic assumption, the gas-uptake data for DCM was best fitted with an additional linear component, later ascribed to GST using *in vitro* results for rodents.

The two-pathway assumption for DCM metabolism with its related PBPK models have been suggested as a valid application for risk assessment purposes (Andersen et al., 1987; David et al., 2006; Marino et al., 2006). In addition, the switch to GSH/GST metabolism at high exposures has been used to assert that because the contribution of this metabolic pathway to total metabolism is numerically very small at low dose, so is the potential risk, particularly for cancer. In addition, the reliance on GSH/GST as the metabolic pathway responsible for toxicity placed in doubt the relevance of human exposures, since humans are rarely exposed to high concentrations. Much of this discussion has centered around the relevance of liver tumor data in rodents. However, in this context, the importance of existing epidemiologic data needs to be examined, particularly with respect to rare tumor occurrences in rodents.

Epidemiologic studies have been limited by small numbers of exposed cases, with few studies able to evaluate exposure–response relationships. However, excess cancers of the pancreas, breast, brain, cervix, prostate, liver, and bile duct, non-Hodgkin's lymphoma; and multiple myeloma have been reported to be associated with DCM exposure (Ruder, 2006). Most of the tumor sites of interest are rare or uncommon tumors. The available cohort studies do not provide the power to detect these tumors, and few studies included adequate

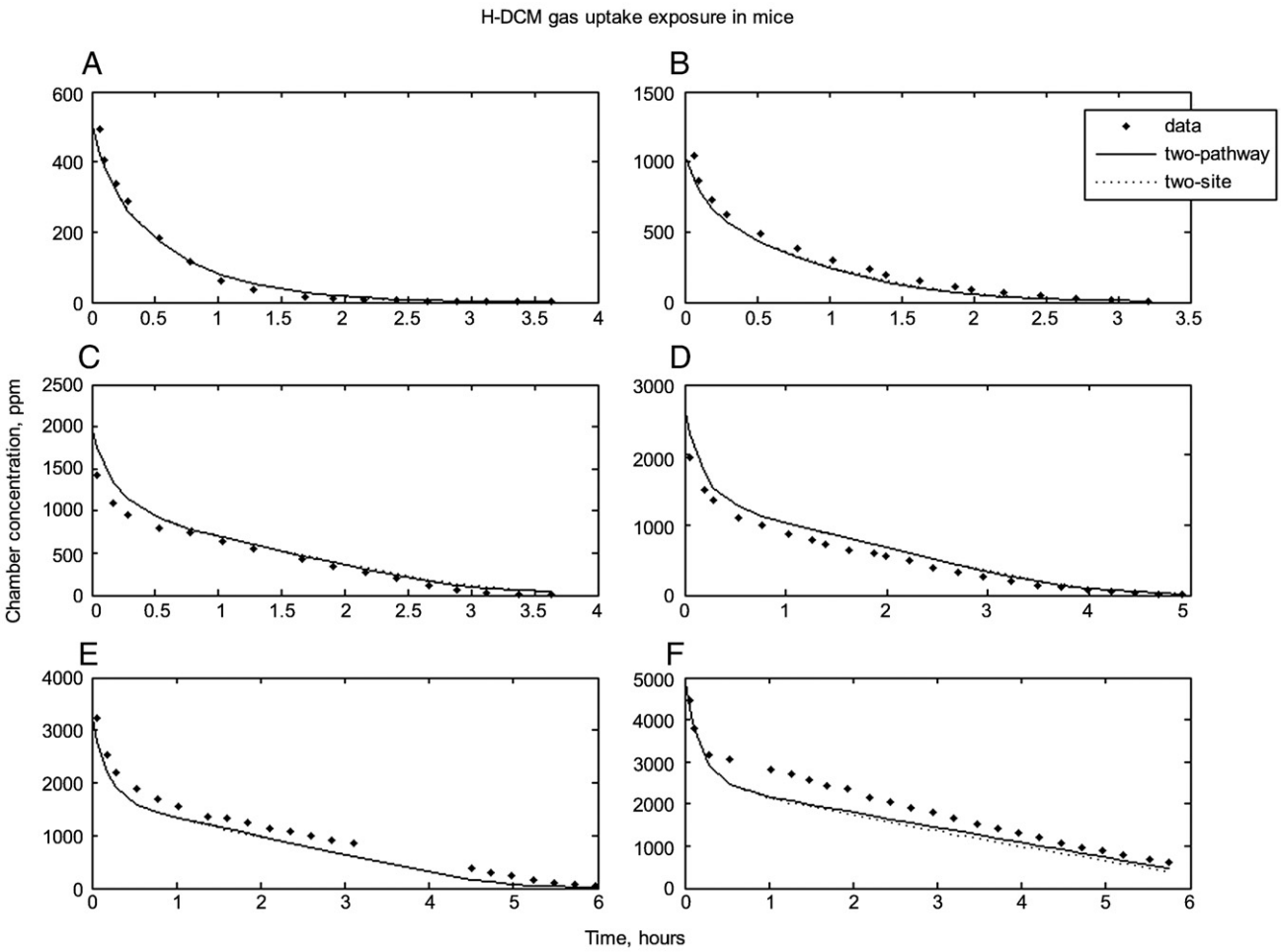

Fig. 4. PBPK modeling results for each H-DCM (normal isotope) gas-uptake concentration. Each panel represents an independent gas-uptake experiment labeled A–F. The dots represent actual experimental data. The solid line presents results for the PBPK model using Eq. (1). The dotted line presents results for the PBPK model using Eq. (2), with all other conditions being the same between models. Note that both simulation results give similar predictions, and therefore generally appear as one line.

numbers of women and, thus, an ability to determine potential excess risk of breast cancer. This is especially important because mammary tumors have also been observed in DCM-exposed rats. The multiple endpoints in both rodents and limited data in humans are suggestive of multiple MOAs for DCM tumor induction.

Glutathione conjugation was estimated by Gargas et al. (1986) to account for 30% of *in vivo* formation of CO_2 in rats using gas uptake data. Watanabe and Guengerich (2006) have shown that this estimation is not tenable due to lack of reactivity of formyl chloride and that another explanation is needed to account for CO_2 formation. Significant mass flux via GSH after P450 oxidation is therefore not likely. The PBPK model by Gargas et al. (1986) assumed a split in total metabolism from modeling of rat gas uptake data that had a linear component that was proportional to the DCM concentration in the organ clearing the parent compound (e.g., liver or lung). This model did not address the mass-balance issues posed by the two hypothesized GSH pathways (i.e., one that Guengerich has shown not to be tenable and the other occurring through direct metabolism of DCM by GST). Although the GST metabolic rate of DCM metabolism is much lower than that of the oxidative pathway, this smaller portion can be biologically relevant to DCM's mode of action for toxicity if it leads formation of a potent metabolite. Guengerich's laboratory was involved in the determination that DCM metabolism via bacterial GST-5 from the rat leads to increased base-pair mutations *in vitro*, and the assumption was made that the *in vitro* results were applicable to those *in vivo* (i.e., mutagenic metabolites are also generated *in vivo*). However, the more recent data from that laboratory tested this assumption and examined GSH-related DNA adduct formation in the livers of mice and rats (Watanabe et al., 2007). Since the GST metabolism is assumed to be linear, it would be expected to produce very small amounts of DNA adducts from reactive GSH metabolites at the concentrations tested. However, there were none found *in vivo* in the livers of mice or rats after DCM exposure (detection level>1 adduct/10^5 nucleotides). As Watanabe et al. (2007) point out, whether the GST pathway could lead to DNA damage at very high concentrations (i.e., those in which the metabolic switch has taken place) is possible but had not been tested.

Given that the rate through the GST pathway is small at both low and high exposure concentration, biological information about the toxicity of DCM needs to be further examined. Experimental evidence for genotoxicity indicates manipulation of the GST pathway can alter toxicity (i.e., increased metabolism via the GSH/GST pathway results in greater genotoxicity in bacterial assays). Nevertheless, DCM is positive in a number of *Salmonella typhimurium* strains for mutagenicity with and without addition of exogenous metabolic activation. The Landi et al. (2003) study analyzed the induction of DNA strand breaks by a number of trihalomethanes using primary lung epithelial cell tissue cultures derived from four human subjects. Two of the subjects were *GST* + and two were *GST* − (see Table 4). However, *GST* activity in all cultures was essentially absent, and there was no correlation with DNA damage and GST genotype. Results for DCM were consistent with bromodichloromethane, bromoform, and chloroform in that there was a dose-

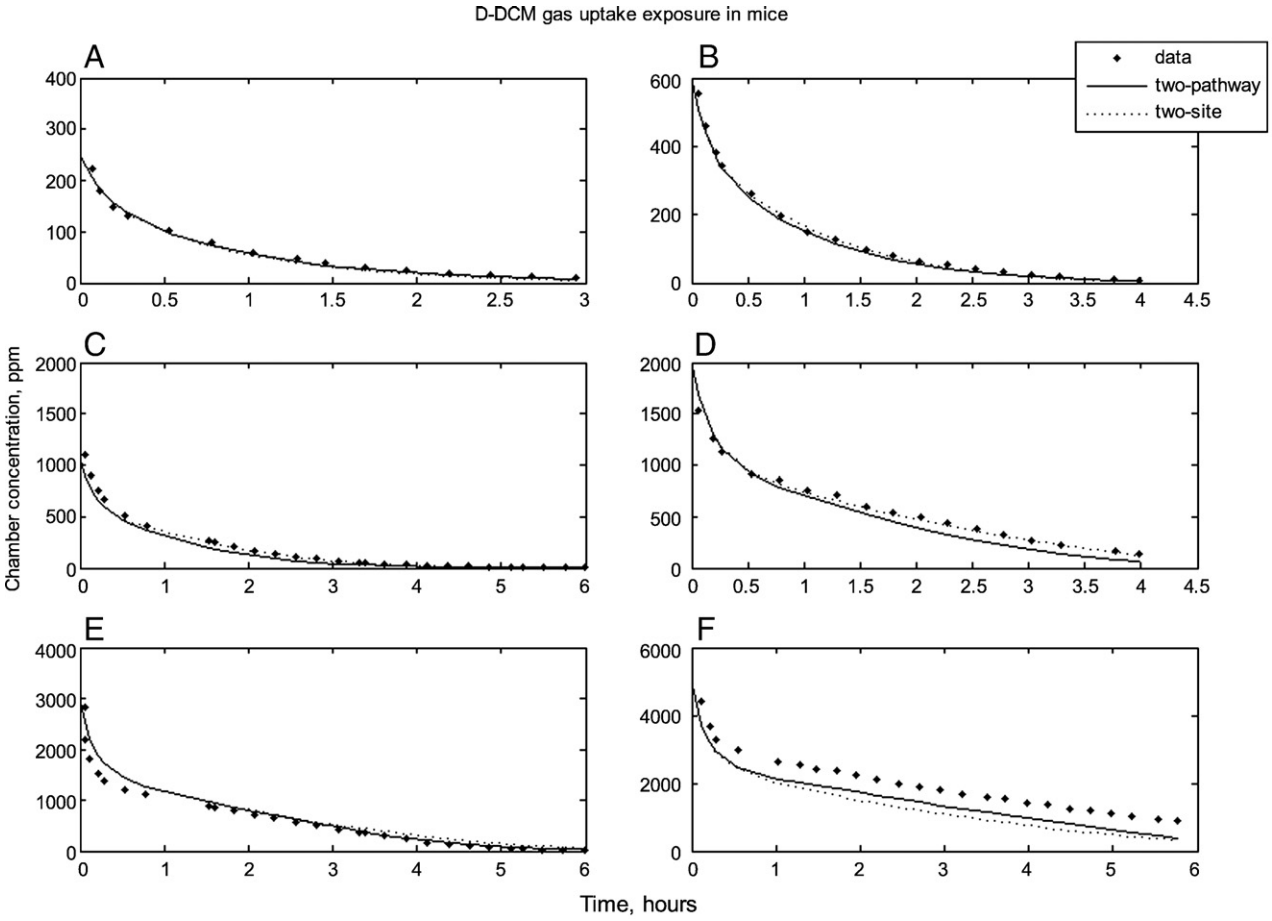

Fig. 5. PBPK modeling results for each D-DCM (heavy or deuterated) gas-uptake concentration. Each panel represents an independent gas-uptake experiment labeled A–F. The dots represent actual experimental data. The solid line presents results for the PBPK model using Eq. (1). The dotted line presents results for the PBPK model using Eq. (2), with all other conditions being the same between models. Note that both simulation results give similar predictions and therefore generally appear as one line.

related increase in comet assay tail extent moments that was not related to the GSTT1-1 status of the individuals or to its activity at all. Of the four datasets, 10, 100, and 1000 μg/l exposures ($n=5$ slides per exposure group) induced a similar dose-response pattern for DCM and chloroform with the tissue cultures derived from the same two individuals providing the greatest response. Activity in half of this limited sample is suggestive of GST-independent DNA damage and that this damage was dose-related. Therefore toxicity from DCM exposure can also be GST-independent.

Not only can PBPK modeling be used to give insight in regards to *in vivo* metabolism, but it can also be used to estimate the concentrations of DCM entering the liver after either inhalation or oral exposure. This information can be used to give context for the exposure concentrations at which the observed metabolic switch (i.e., concentration range over which metabolic rates changed) occurs and the differences between what can be observed *in vivo* and what has been used in *in vitro* paradigms to characterize GST activity and to make implications regarding risk assessment. For inhalation exposure, our figures show that the concentration in the range of 1700 ppm is the exposure in which changes in metabolic rates are evident using inhalation gas uptake data. Using the PBPK model, at 1700 ppm, the DCM concentration going into the liver was estimated to be 0.24 mM. The inhalation model was modified for oral exposure using the two-pathway model (the two-site model gives the same results) with aqueous media used as the vehicle for gavage. One additional constant was incorporated in this model, that of absorption from the stomach or ka of 0.3 (h^{-1}). The equivalent oral bolus dosing concentration needed to produce 0.24 mM DCM going into the liver was predicted to be 470 mg/kg. The context of several *in vitro* results is readily apparent from these estimates.

An important issue raised by this paper is that if CYP2E1 is capable of being responsible for the metabolic shift observed around 1700 ppm, what contribution if any can GST-T1 make to DCM metabolism under *in vivo* conditions? Reitz et al. (1989) provided *in vitro* estimates of DCM metabolism through the P450 and GST-T1 (or their analogues) pathways in mice, rats, and humans and noted that the K_Ms for this form of GST in the livers of all species were over 40 mM. The velocity vs. substrate curves were linear. The *in vitro* findings of Reitz et al. (1989) suggested that P450 enzymes were much more efficient than that of GST-T1 for DCM metabolism. Using K_M and V_{max} to estimate clearance, there is at least 10-fold greater efficiency for DCM clearance by the liver by the P450 system than the GST pathway. However, the lowest concentrations used to determine DCM metabolism by the P450 system *in vitro* was 1 mM and past the point in which the metabolic switch would occur. This could result in an underestimate of P450 activity *in vitro* and thus the efficiency of the P450 system over the GST pathway could be even greater. Reitz et al. (1989) noted that the *in vitro* derived K_M values for the P450s were as much as two orders of magnitude higher than those observed *in vivo* derived by PBPK models, even after accounting for correction for DCM lost in the headspace of *in vitro* assays and the difference in what the *in vivo* estimates represent. The *in vitro* GST–T1 data show that its activity would not be affected by saturation of the enzyme, but more importantly that very large concentrations were needed to record any such activity (i.e., the lowest concentration used was 6.7 mM DCM). The concentration in which the metabolic switch occurs *in vivo* is at least 25-fold lower than that in which GST activity

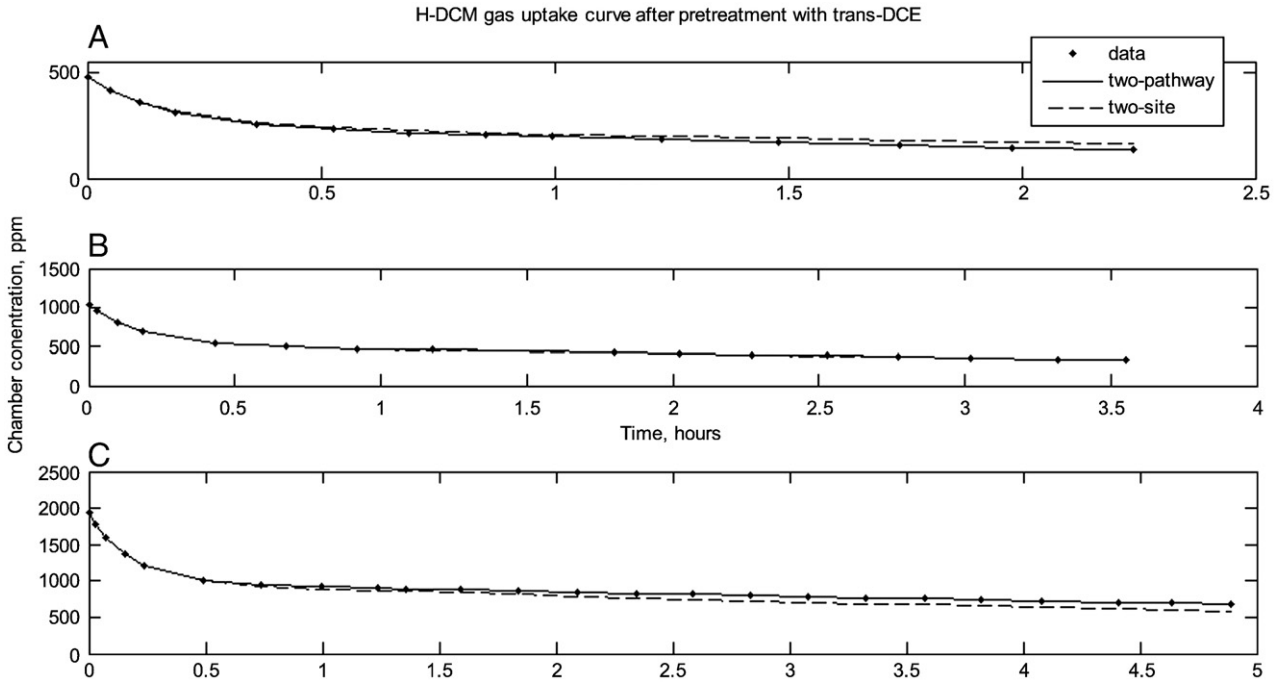

Fig. 6. PBPK modeling results for each H-DCM pretreated with inhibitor trans-DCE gas-uptake concentration experiments. Each panel represents an independent gas-uptake experiment labeled A–C. The dots represent actual experimental data. The solid line presents results for the PBPK model using Eq. (1). The dotted line presents results for the PBPK model using Eq. (2), with all other conditions being the same between models. Note that both simulation results give similar predictions, and therefore generally appear as one line.

was observed *in vitro*. Thus, it is likely that *in vivo* the GST–T1 pathway cannot compete with the P450 pathway for DCM metabolism in the mouse, rat, or human.

Another aspect of our analyses is the relationship of our *in vivo* V_{max} and K_M estimates to previous studies. The K_M values obtained in this paper for the two-pathway model in female mice compare favorably with previous estimates of 1.34 mg/l in mice (Clewell et al., 1993). Given that the K_M estimates for female mice in our analyses are close to previously estimated values, the suggestion can be made that changes introduced in our updated two-pathway model are minor. Since we are proposing the two-site hypothesis for the first time, there are no previous estimates of either V_{max} or K_M for a second CYP2E1 site. Given that K_M is more difficult to estimate than V_{max}, the decision was made to use the clearance ratio for the second binding site postulated to occur with the two-site model (Evans and Andersen, 1995). In this way, we were able to minimize the number of regression parameters needed for optimization. In this case, the implicit assumption is made that K_M2 is much bigger than K_M1, an assumption that helps explain the resulting shallow slope for the second phase observed after the proposed metabolic switch occurs. This shallower slope is consistent with the velocity plots presented in Figs. 8 and 9 and is an integral component of the two-site one pathway hypothesis.

Other than assumptions regarding GST metabolism of DCM being responsible for the metabolic shift, data that have used to support a role for GST metabolism of DCM *in vivo* is the use of radiolabeled DCM administration and the relative ratios of CO and CO_2 resulting in exhaled breath (Angelo et al., 1986a,b; Kirschman et al., 1986). The P450 pathway was assumed to produce CO and the GST pathway CO_2. In the Angelo et al. (1986a,b) studies, radiolabeled CO_2 levels were reported to be higher than those of radiolabeled CO in both mice and rats after single exposures, and CO_2 formation showed saturation with dose in rats and mice. The apparent saturation of CO_2 formation is inconsistent with the linear kinetics of DCM metabolism through the GST pathway. The excessive CO_2 formation has been attributed to formyl chloride reactivity with GSH to form CO_2. However, Watanabe and Guengerich (2006) show this does not occur. The excess radiolabeled CO_2 observed in these studies is also inconsistent with the much lower ability of this pathway to metabolize DCM than that of the P450 system under physiologic conditions described above.

In the review by Kirschman et al. (1986), a figure is presented for combined CO and CO_2 detection through exhalation. Although it is impossible to separate CO from CO_2, this data matches the velocity plots for the two-site one pathway model described in this paper for metabolism through only the P450 pathway. Humans have GST–T1 activity expressed in red blood cells with similar K_M and V_{max} as that expressed in liver (Hallier et al., 1994; Reitz et al., 1989). However, rats do not have this form of GST expressed in their red blood cells (Hallier et al., 1994) and such activity has not been reported in mice. Therefore, the excess CO_2 observed in rats after DCM exposure cannot be attributed to extrahepatic GST metabolism by red blood cells.

Guengerich et al., (2003) used pure GST (rat and human) in bacteria (*E. coli*) and saw no kinetic burst in the reaction for DCM metabolism that has been observed in bacterial versions of the enzyme. This study confirmed the apparent low affinity (high K_M) of mammalian GST for DCM, similar to the reports of Reitz et al. (1989). Thier et al. (1993) reported increased revertants after DCM exposure in *S. typhimurium* TA1535 possessing GST 5-5 from rat but got a much lower response at higher concentrations than in similar assays of ethylene dibromide, CH_2Br_2, and CH_2BrCl. The lowest concentration of DCM used was 0.2 mM and the response peaked at 1 mM. The modest responses (i.e., at most a doubling over background rate) were at concentrations in which the enzyme has been shown *in vitro* to have very little ability to compete with P450 for DCM metabolism. However, the positive response in +GST 5-5 bacteria was at the same range of *in vitro* DCM concentrations in which Landi et al. (2003) reported positive results for lung cells derived from an individual donor with no GSTT-1 activity (i.e., number C).

Finally, as noted by Watanabe et al. (2007), no adducts were found in mice exposed to 5 mg/kg radiolabeled DCM through i.p. injection. The oral route of exposure would be the most analogous to this route of exposure. Although methods for DNA adduct detection were very sensitive and the GST activity is expected to be linear, the lack of finding of adducts is consistent with the inability of GST to compete with P450

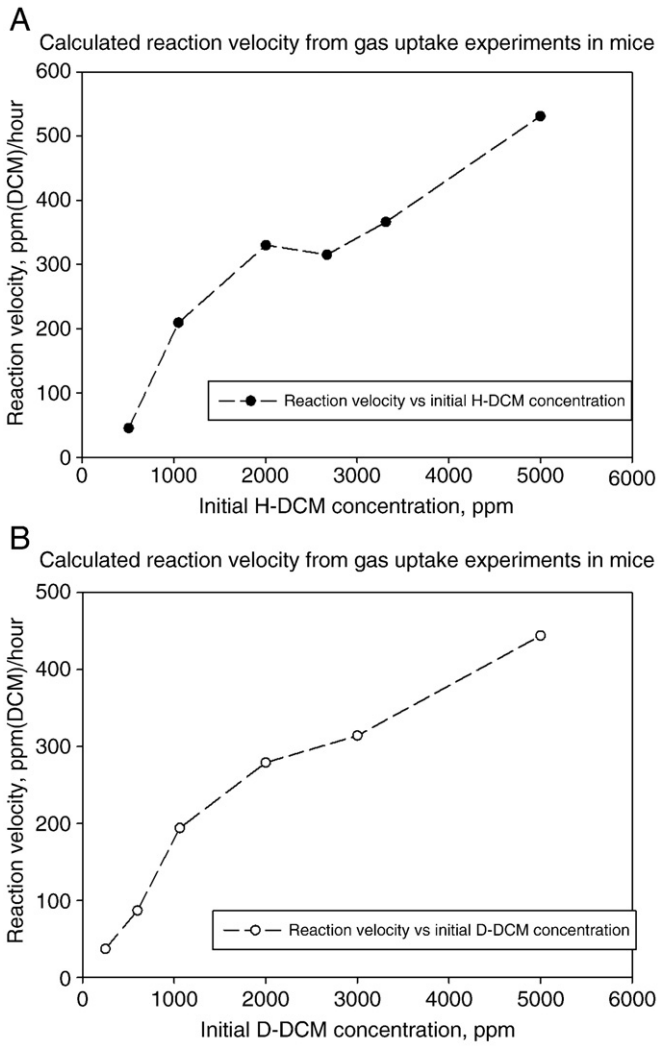

Fig. 7. (A) Calculated slope from experimental H-DCM gas-uptake data at the end of 2 h. The slope was calculated at the end of two hours for different initial concentrations (*x* axis). (B) Calculated slope from experimental D-DCM gas-uptake data at the end of 2 h. The slope was calculated at the end of two hours for different initial concentrations (*x* axis),

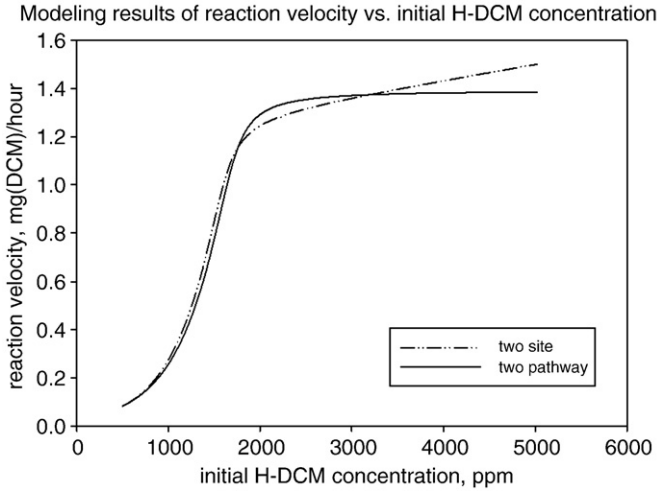

Fig. 8. Predictions of slope calculated at the end of 2 h for two different metabolic models for H-DCM gas-uptake exposure while varying initial exposure concentrations.

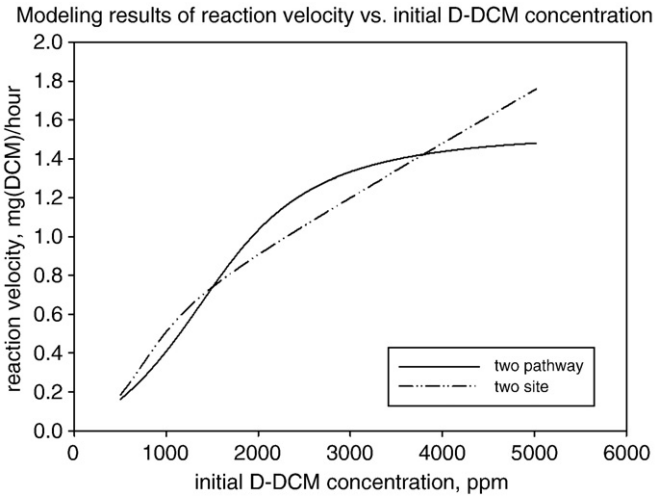

Fig. 9. Predictions of slope calculated at the end of 2 h for two different metabolic models for D-DCM gas-uptake exposure while varying initial exposure concentrations.

for DCM metabolism at a dose our PBPK model has shown to be well below the metabolic switching point.

Recent information has shown that several CYPs have shown atypical kinetic behavior (Tracy, 2006). This atypical behavior is possible due to expansion of the active site to include multiple ligands and the description of two-site due to these multiple binding sites. The behavior of one enzyme can, therefore, be used to account for a biphasic behavior with different metabolic rates for increasing exposure concentrations. One of these atypical kinetic behaviors fitting the description of a metabolic switch has been identified for several P450s: CYP3A4 (Korzekwa et al., 1998) and suggested for CYP2E1 (Harrelson et al., 2008). Because two sites can explain the metabolic switch profile for DCM metabolism using only one enzyme (CYP2E1), a re-examination of the gas-uptake data was warranted. As shown by our analysis, the two-pathway model can be compared to one using two-sites in one enzyme as an alternate kinetic mechanism. Future research can then help identify the implications of this alternate view for potential MOA(s).

Porubsky et al. (2008) have studied the crystallized structure of human CYP2E1 in order to gain insights as to how this enzyme can simultaneously metabolize small molecules and large molecules, such as fatty acids. These authors describe an access channel that can be directly connected to the active site via rotation of Phe atoms. This direct access would allow ligand or solvent access or exit and enhance the metabolic ability of the active site. This conformational change in CYP2E1 and related change in metabolic capacity is exactly what the two-site rate equation describes. The newly acquired knowledge of the human CYP2E1 structure is entirely consistent with the gas uptake re-analysis presented in this paper. The CYP2E1 molecule is actually designed to allow for this metabolic switching to occur at higher concentrations. Finally, one major contribution of the current effort is to highlight the ability of the gas-uptake inhalation to describe this level of structural detail when used in combination with PBPK modeling.

Table 4
DNA damage induced by DCM in human lung cells (results from Landi et al., 2003).

Concentration (μM)	GSTT1-1 genotype	Tail extent moment ± SE[a]
10	−	7.1 ± 1.91
10	+	8.1 ± 1.85
100	−	13.7 ± 1.91[b]
100	+	11.5 ± 1.90
1000	−	15.3 ± 1.90[b]
1000	+	10.4 ± 1.96

[a] Data are pooled from two GSTT1-1− subjects and two GSTT1-1+ subjects. Control tail extent moment ± SE > were 10.0 ± 0.85 for GSTT1-1− and 8.8 ± 0.88 for GSTT1-1+.
[b] Significant differences compared to controls ($P<0.05$).

Another gas-uptake inhalation dataset included in the present analysis was the deuterated DCM data set partially published by Andersen et al. (1994). In the previous analysis (Andersen et al., 1994), only the two lowest concentrations were analyzed. However, in order to observe metabolic switching, the full range of concentrations needs to be included, as we have shown. The velocity plot analysis of the deuterated data presented in Fig. 9 and related simulations show that although deuteration alters metabolism, that such data also cannot distinguish between the two-site and two-pathway models. These analyses of several types of data strengthen the observation that both models are supported by the existing PBPK data.

One potential question that can also be addressed concerns the ability of i.v. experiments to estimate metabolic parameters, particularly metabolism in the lung. When using i.v. exposure via the tail vein, the lung becomes the first major organ to clear DCM. Since the lung is a target of DCM toxicity, GST metabolism of DCM has been suggested to be involved in lung carcinogenicity. Angelo et al. (1984) collected venous concentration time course data after i.v. exposure to 10 and 50 mg/kg of DCM in mice. The PBPK model was modified to include a lung compartment and compared to i.v. *in vivo* data as an additional route of exposure (data not shown). When using both metabolic hypotheses, the addition of this parameter and comparison to the i.v. data was unable to further distinguish between the two metabolic hypotheses. A possible explanation for this behavior consists of the venous compartment becoming a mixture chamber for venous blood coming in from different organs. As the fat, liver, and slowly and rapidly perfused venous blood combined compartments are combined in the venous compartment, information content due to metabolism from the liver is minimized.

Finally, an additional test was performed by the incorporation of an inhibition parameter in the model and using a combined optimization of naïve and trans-DCE pre-treated data. The inhibition parameter represents the available concentration of CYP2E1.[1] Our results of the combined naïve and trans-DCE optimization at various concentrations found the inhibition fraction to be consistently 0.15 for both metabolic models. That is, if the naïve treatment represents 100% of V_{max}, then trans-DCE inhibition is described by 15% of V_{max} left, or 85% inhibition, regardless of the metabolic model used. These results are consistent with Mathews et al. (1998) who reported a maximum *in vivo* inhibition of 64% in rats and mice specifically affecting CYP2E1 after dosing trans-DCE at various concentrations ("A dose of 100 mg/kg produced a 64% loss of P4502E1 activity that was greater than the 25 and 50 mg/kg doses, but not statistically different from the 400 and 800 mg/kg doses."). These animals were dosed once and sacrificed 5 h after administration of trans-DCE. For our analysis, gas-uptake pre-treated animals were immediately followed by DCM exposure, so a direct comparison with Mathews' inhibition experiments is not possible, since the experimental paradigms were different. Lilly et al. (1998) used PBPK modeling to try and distinguish between four different inhibition mechanisms for trans-DCE (i.e., reactive metabolite reacts with enzyme-substrate (ES) complex, reactive metabolite reacts with total enzyme present, reactive metabolite reacts with free enzyme, and bound intermediate inactivates enzyme in a first-order process). A mathematical index was used to infer which CYP2E1 inactivation model provided the best fit to the gas-uptake data. Lilly et al. (1998) concluded that trans-DCE is a potent inhibitor, but this work was not able to distinguish between irreversible and reversible binding or the possibility of two binding sites. These results suggest a gap in the literature confirming the validity of trans-DCE as a complete inhibitor of CYP2E1 and the nature of that inhibition and thus different sets of mechanistic *in vivo* experiments need to be performed.

A clarification is warranted for use of the term "switch" in the context of the metabolic phenomenon being described in this paper and other concepts. The metabolic switch is not a "dose transition" in which there could be a threshold in dose–response as one process could be completely turned off as another begins at a higher dose or another process only occurs a the higher dose. The two-site binding model is not such a transition model and neither is the two-pathway model. For the two-site model, once the substrate is in place and a conformational change takes place in CYP2E1, then the second site is available for binding. Both sites are available at the same time and the binding process can occur in parallel. The clearance values of each site are determined by the binding of the substrate to both sites and the velocity of the reaction is described by a curve with two slopes. Thus, the two-site binding model describes the gas uptake data as a reflection of both binding sites acting in parallel and no assumption of a "dose transition". Similarly, the original Andersen et al. PBPK model (Andersen et al., 1987) and its descendents, that assume a two-pathway model for DCM metabolism, do not have a dose transition or switch, but predict a higher proportion of GST metabolism at high doses versus low so that there is a continuous dose–response relationship rather than threshold of effect.

In summary, the application of PBPK modeling to gas-uptake data in mice has demonstrated that two different metabolic hypotheses can fit the same data. This modeling approach provides support that is consistent with an alternate metabolic hypothesis for DCM. Our current analysis demonstrated the two-site within one enzyme to be consistent with the concept of a metabolic switch at higher concentrations for DCM metabolism. Further analysis using the PBPK model described here to estimate *in vivo* concentrations at the metabolic switching point and an examination of *in vitro* metabolism of DCM through the GST–T1 pathway suggests that GST–T1 (or its analogues in rodents) is unable to compete with the P450 pathway. Inferences regarding the carcinogenesis of dichloromethane should include the current concepts in CYP2E1 kinetic mechanisms.

Disclaimer

This manuscript has been reviewed by the U.S. Environmental Protection Agency and approved for publication. The views expressed in this manuscript are those of the authors and do not necessarily reflect the views or policies of the U.S. Environmental Protection Agency.

Acknowledgments

The authors would like to thank Drs. David DeMarini and Weihsueh Chiu for helpful comments during the preparation of this manuscript. Special thanks to Dr. Edward Croom for suggesting inclusion of recent CYP2E1 data. This work would have not been possible without the technical support of Mr. Christopher Eklund, who kindly digitized all the available gas uptake data.

Appendix A. Supplementary data

Supplementary data associated with this article can be found, in the online version, at doi:10.1016/j.taap.2010.01.018.

References

Anders, M.W., 2008. Chemical toxicology of reactive intermediates formed by the glutathione-dependent bioactivation of halogen-containing compounds. Chem. Res. Toxicol. 21, 145–159.

Andersen, M.E., Clewell III, H.J., Gargas, M.L., Smith, F.A., Reitz, R.H., 1987. Physiologically based pharmacokinetics and the risk assessment process for methylene chloride. Toxicol. Appl. Pharmacol. 87, 185–205.

[1] An inhibition constant theta, assumed to be a fraction of the naïve data was multiplied by V_{max} in both metabolic equations. Theta was assumed to be one for the naïve dataset. Theta was found to be 0.15 of V_{max} when using the trans-DCE pretreated data for both metabolic hypotheses.

Andersen, M.E., Clewell III, H.J., Mahle, D.A., Gearhart, J.M., 1994. Gas uptake studies of deuterium isotope effects on dichloromethane metabolism in female B6C3F1 mice in vivo. Toxicol. Appl. Pharmacol. 128, 158–165.

Angelo, M.J., Bischoff, K.B., Pritchard, A.B., Presser, M.A., 1984. A physiological model for the pharmacokinetics of methylene chloride in B6C3F1 mice following i.v. administrations. J. Pharmacokinet. Biopharm. 12, 413–436.

Angelo, M.J., Pritchard, A.B., Hawkins, D.R., Waller, A.R., Roberts, A., 1986a. The pharmacokinetics of dichloromethane: I. Diposition in B6C3F1 mice following intravenous and oral administration. Food Chem. Toxicol. 24 (9), 965–974.

Angelo, M.J., Prichard, A.B., Hawkins, D.R., Waller, A.R., Roberts, A., 1986b. The pharmacokinetics of dichloromethane: II. Disposition in Fischer 344 rats following intravenous and oral administration. Food Chem. Toxicol. 24 (9), 975–980.

Atkins, G.L., Nimmo, I.A., 1973. The reliability of Michaelis constants and maximum velocities estimated by using the integrated Michaelis–Menten equation. Biochem. J. 135, 779–784.

Brown, R.P., Delp, M.D., Lindstedt, S.L., Rhomberg, L.R., Beliles, R.P., 1997. Physiological parameter values for physiologically based pharmacokinetic models. Toxicol. Ind. Health 13, 407–484.

Clewell, H.J., III, Gearhart, J.M., and Andersen, M.E. (1993). Analysis of the metabolism of methylene chloride in the B6C3F1 mouse and its implications for human risk assessment. Submission to OSHA 96.

David, R.M., Clewell, H.J., Gentry, P.R., et al., 2006. Revised assessment of cancer risk to dichloromethane II. Application of probabilistic methods to cancer risk determinations. Regul. Toxicol. Pharmacol. 45, 55–65.

El-Masri, H.A., Dowd, S.M., Pegram, R.A., Harrison, R.A., Yavanhxay, S., Simmons, J.E., Evans, M.V., 2009. Development of an inhalation physiologically-based pharmacokinetic (PBPK) model for 2,2,4-trimethylpentane (TMP) in male Long Evans rats using gas uptake experiments. Inhal. Toxicol. 21, 1176–1185 DOI:10.3109/08958370903005751.

Evans, M.V., Andersen, M.E., 1995. Sensitivity analysis and the design of gas uptake inhalation studies. Inhal. Toxicol. 7, 1075–1094.

Evans, M.V., Chiu, W.A., Okino, M.S., Caldwell, J.C., 2009. Development of an updated PBPK model for trichloroethylene and metabolites in mice, and its application to discern the role of oxidative metabolism in TCE-induced hepatomegaly. Toxicol. Appl. Pharmacol. 236, 329–340.

Gargas, M.L., Clewell III, H.J., Andersen, M.E., 1986. Metabolism of inhaled dihalomethanes in vivo: differentiation of kinetic constants for two independent pathways. Toxicol. Appl. Pharmacol. 82, 211–223.

Guengerich, F.P., Kim, D.H., Iwasaki, M., 1991. Role of human cytochrome P-450 IIE1 in the oxidation of many low molecular weight cancer suspects. Chem. Res. Toxicol. 4, 168–179.

Guengerich, F.P., McCormick, W.A., Wheeler, J.B., 2003. Analysis of the kinetic mechanism of haloalkane conjugation by mammalian theta-class glutathione transferases. Chem. Res. Toxicol. 16, 1493–1499.

Halllier, E., Schröder, K.R., Asmuth, K., Dommermuth, A., Aust, B., Werner Goergens, H., 1994. Metabolism of dichloromethane (methylene chloride) to formaldehyde in human erythrocytes: influence of polymorphisms of glutathione transferase Theta (GST T1-1). Arch. Toxicol. 68, 423–427.

Harrelson, J.P., Atkins, W.M., Nelson, S.D., 2008. Multiple-ligand binding in CYP2A6: probing mechanisms of cytochrome P450 cooperativity by assessing substrate dynamics. Biochemistry 47, 2978–2988.

Harrelson, J.P., Henne, K.R., Alonso, D.O., Nelson, S.D., 2007. A comparison of substrate dynamics in human CYP2E1 and CYP2A6. Biochem. Biophys. Res. Commun. 352, 843–849.

Hazelton Laboratories, (1983) 24-Month oncogenicity study of methylene chloride in mice [final report]. Performed by Hazelton Laboratories America, Inc., Vienna, VA for the National Coffee Association, New York, NY; Submitted under TSCA Section 4; EPA Document No. 45-8303005; NTIS No. OTS0206132.

IARC (International Agency for Research on Cancer), (1999) Dichloromethane. IARC monographs on the evaluation of carcinogenic risk of chemicals to humans. Vol. 71. Re-evaluation of some organic chemicals, hydrazine and hydrogen peroxide. Lyon, France: International Agency for Research on Cancer, pp. 251–315. Available online at http://inchem.org/documents/iarc/vol71/004-dichloromethane.html.

Kirschman, J.C., Brown, N.M., Coots, R.H., Morgareidge, K., 1986. Review of investigations of dichloromethane metabolism and subchronic oral toxicity as the basis for the design of chronic oral studies in rats and mice. Food Chem. Toxicol. 24 (9), 943–949.

Korzekwa, K.R., Krishnamachary, N., Shou, M., Ogai, A., Parise, R.A., Rettie, A.E., Gonzalez, F.J., Tracy, T.S., 1998. Evaluation of atypical cytochrome P450 kinetics with two-substrate models: evidence that multiple substrates can simultaneously bind to cytochrome P450 active sites. Biochemistry 37, 4137–4147.

Landi, S., Naccarati, A., Ross, M.K., Hanley, N.M., Dailey, L., Devlin, R.B., Vasquez, M., Pegram, R.A., DeMarini, D.M., 2003. Induction of DNA strand breaks by trihalomethanes in primary human lung epithelial cells. Mutat. Res. 538, 41–50.

Lilly, P.D., Thornton-Manning, J.R., Gargas, M.L., Clewell, H.J., Andersen, M.E., 1998. Kinetic characterization of CYP2E1 inhibition in vivo and in vitro by the chloroethylenes. Arch. Toxicol. 72, 609–621.

Maltoni, C., Cotti, G., Perino, G., 1988. Long-term carcinogenicity bioassays on methylene chloride administered by ingestion to Sprague-Dawley rats and Swiss mice and by inhalation to Sprague-Dawley rats. Ann. N.Y. Acad. Sci. 534, 352–366.

Marino, D.J., Clewell, H.J., Gentry, P.R., Covington, T.R., Hack, C.E., David, R.M., Morgott, D.A., 2006. Revised assessment of cancer risk to dichloromethane: Part I. Bayesian PBPK and dose-response modeling in mice. Regul. Toxicol. Pharmacol. 45, 44–54.

Mathews, J.M., Etheridge, A.S., Raymer, J.H., Black, S.R., Pulliam Jr, D.W., Bucher, J.R., 1998. Selective inhibition of cytochrome P450 2E1 in vivo and in vitro with trans-1,2-dichloroethylene. Chem. Res. Toxicol. 11, 778–785.

Mennear, J.H., McConnell, E.E., Huff, J.E., et al., 1988. Inhalation and carcinogenesis studies of methylene chloride (dichloromethane) in F344/n rats and B6C3F$_1$ mice. Ann. N.Y. Acad. Sci. 534, 343–351.

Nitschke, K.D., Burek, J.D., Bell, T.J., et al., 1988. Methylene chloride: a 2-year inhalation toxicity and oncogenicity study in rats. Fundam. Appl. Toxicol. 11, 48–59.

NTP (National Toxicology Program), 1986. Toxicology and carcinogenesis studies of dichloromethane (methylene chloride) (CAS No. 75-09-2) in F344/N rats and B6C3F1 mice (inhalation studies). Natl. Toxicol. Program Tech. Rep. Ser. 306, 1–208.

Porubsky, P.R., Meneely, K.M., Scott, E.E., 2008. Structures of human cytochrome P-450 2E1. Insights into the binding of inhibitors and both small molecular weight and fatty acid substrates. J. Biol. Chem. 283, 33698–33707. Electronic publication 2008. Sep. 24.

Ramsey, J.C., Andersen, M.E., 1984. A physiologically based description of the inhalation pharmacokinetics of styrene in rats and humans. Toxicol. Appl. Pharmacol. 73, 159–175.

Reitz, R.H., Mendrala, A.L., Guengerich, F.P., 1989. *In vitro* metabolism of methylene chloride in human and animal tissues: use in physiologically based pharmacokinetic models. Toxicol. Appl. Pharmacol. 97, 230–246.

Ruder, A.M., 2006. Potential health effects of occupational chlorinated solvent exposure. Ann. N. Y. Acad. Sci. 1076, 207–227.

Segel, I.H., 1993. Enzyme kinetics: Behavior and Analysis of Rapid Equilibrium and Steady-State Enzyme Systems. Wiley Classics, New York.

Serota, D.G., Thakur, A.K., Ulland, B.M., et al., 1986a. A two-year drinking water study of dichloromethane in rodents: I. Rats. Food. Chem. Toxicol. 24 (9), 951–958.

Serota, D.G., Thakur, A.K., Ulland, B.M., et al., 1986b. A two-year drinking water study of dichloromethane in rodents: II. Mice. Food. Chem. Toxicol. 24 (9), 959–963.

Slikker Jr., W., Andersen, M.E., Bogdanffy, M.S., Bus, J.S., Cohen, S.D., Conolly, R.B., David, R.M., Doerrer, N.G., Dorman, D.C., Gaylor, D.W., Hattis, D., Rogers, J.M., Woodrow Setzer, R., Swenberg, J.A., Wallace, K., 2004. Dose-dependent transitions in mechanisms of toxicity. Toxicol. Appl. Pharmacol. 201, 203–225.

Sweeney, L.M., Kirman, C.R., Morgott, D.A., Gargas, M.L., 2004. Estimation of interindividual variation in oxidative metabolism of dichloromethane in human volunteers. Toxicol. Lett. 154, 201–216.

Thier, R., Taylor, J.B., Pemble, S.E., Humphreys, W.G., Persmark, M., Ketterer, B., Guengerich, F.P., 1993. Expression of mammalian glutathione S-transferase 5-5 in *Salmonella typhimurium* TA1535 leads to base-pair mutations upon exposure to dihalomethanes. Proc. Natl. Acad. Sci. U. S. A. 90, 8576–8580.

Tracy, T.S., 2006. Atypical cytochrome p450 kinetics: implications for drug discovery. Drugs R. D. 7, 349–363.

Watanabe, K., Guengerich, F.P., 2006. Limited reactivity of formyl chloride with glutathione and relevance to metabolism and toxicity of dichloromethane. Chem. Res. Toxicol. 19, 1091–1096.

Watanabe, K., Liberman, R.G., Skipper, P.L., Tannenbaum, S.R., Guengerich, F.P., 2007. Analysis of DNA adducts formed in vivo in rats and mice from 1,2-dibromoethane, 1,2-dichloroethane, dibromomethane, and dichloromethane using HPLC/accelerator mass spectrometry and relevance to risk estimates. Chem. Res. Toxicol. 20, 1594–1600.